
Collective Coordinate Methods and Their Applicability to φ^4 Models

Herbert Weigel

Institute for Theoretical Physics, Physics Department, Stellenbosch University,
South Africa
`weigel@sun.ac.za`

Summary. Collective coordinate methods are frequently applied to study dynamical properties of solitons. These methods simplify the field equations - typically partial differential equations - to ordinary differential equations for selected excitations. More importantly though, collective coordinates provide a practical means to focus on particular modes of otherwise complicated dynamical processes. We review the application of collective coordinate methods in the analysis of the kink-antikink interaction within the φ^4 soliton model and illuminate discrepancies between these methods and the exact results from the field equations.

1 Motivation

The φ^4 model represents the simplest non-linear extension of the Klein-Gordon theory in one time and one space dimensions that contains solutions with localized energy densities. These solutions are usually called *solitons* though more precisely they should be named solitary waves [1, 2].

Solitons have applications in almost all disciplines of physics. For example they characterize domains that may emerge in cosmology [3, 4] or in condensed matter [5, 6]. The localized energy densities assign particle structures to solitons and picturing baryons as chiral solitons successfully describes many of their static and dynamic properties [7]. Solitons typically emerge in field theories with degenerate vacua such that the soliton configuration takes different vacuum values in distinct regimes of spatial infinity. When it takes an infinite amount of energy to (continuously) transform these vacuum configurations into another, the so-constructed solitons are named *topological* [8].

The Lagrange density of the φ^4 model in one space and one time dimensions may be written as compactly as

$$\mathcal{L} = \frac{1}{2} [\dot{\varphi}^2 - \varphi'^2] - \frac{1}{2} (\varphi^2 - 1)^2, \quad (1)$$

where dots and primes denote (partial) derivatives with respect to time (t) and space (x) coordinates, respectively. Fields and variables have been scaled such that the self-

interaction strength occurs as an overall constant factor¹ which is not displayed. The degenerate vacua are simply $\varphi_{\text{vac}} = \pm 1$ and there are two options to connect them thereby defining kink and antikink solutions. With the above conventions these are

$$\varphi_{K,\bar{K}}(x) = \pm \tanh(x). \quad (2)$$

The φ^4 model (anti)kink is the prototype soliton that illuminates many of the structures to be expected for the technically more challenging applications mentioned above.

Given that these are solutions within a non-linear model, any superposition of two solutions will, in general, not be a solution anymore. However, a superposition of two widely separated solitons is still approximately a solution as interference contributions to the energy vanish. As the separation is reduced practically adiabatically, the super-imposed configurations will possess some interaction energy. Within the particle interpretation of the soliton, the separation is the distance between two particles and the interaction energy becomes the inter-particle potential [9].

In general this interaction can be studied by solving the time dependent field equations as an initial value problem. Definitely, for models in one space dimension this is an option. But in higher, in particular three, dimensions such computations become increasingly demanding. In that case a possible strategy is the introduction of so-called *collective coordinates* that parameterize certain modes of the field excitations and reduce the complexity of the field equations drastically. Their introduction, to some extent, is a matter of good guess. We are in the lucky situation that for soliton models in one space dimension we can compare the solutions to the exact field equations to those from the reduced equations for the collective coordinates. This comparison will then determine the quality of the guess. Besides these technical advantages, a maybe even more important feature of collective coordinates is that they enable us to focus on special excitations of the soliton. Studying collective coordinates thus not only sheds light on their dynamical relevance but ultimately identifies modes which trigger certain processes thereby deepening our understanding of the particular soliton model. Here we will review this investigation for the kink-antikink system of the φ^4 model.

In the following section we will discuss the dynamics of the kink-antikink interaction resulting from the full field equations. In section 3 we will introduce collective coordinates to (eventually) detail the dynamics of this interaction. In section 4 we will briefly reflect on previous approximations to the collective coordinate approach and discuss one out of many possible generalizations in section 5. Section 6 shows how the collective coordinate approach is applied to the ϕ^6 model. We conclude in section 7 in which we also discuss reasons why the (specific) collective coordinate approach fails to properly describe the kink-antikink interaction.

2 Kink-antikink scattering

Kink-antikink scattering can be simulated as a solution to the field equations with suitable initial conditions. Here we discuss this treatment and its results briefly.

¹ Here we restrain to the classical description, *i.e.* canonical commutation relations are not imposed. Then this factor has no dynamical relevance.

2.1 Dynamical kink-antikink interaction

The field equation emerging from the Lagrangian, Eq. (1) reads

$$\ddot{\varphi} - \varphi'' = 2\varphi(1 - \varphi^2). \quad (3)$$

This field equation is a partial differential equation (PDE) and has a unique solution when the initial field configuration and its time derivative (velocity) are prescribed. The initial conditions suitable to describe the kink-antikink interaction read

$$\begin{aligned} \varphi(x, 0) &= \varphi_{\overline{K}}\left(\frac{x}{\sqrt{1-v^2}} - X_0\right) + \varphi_K\left(\frac{x}{\sqrt{1-v^2}} + X_0\right) - 1, \\ \dot{\varphi}(x, 0) &= \frac{v}{\sqrt{1-v^2}} \left[\varphi'_{\overline{K}}\left(\frac{x}{\sqrt{1-v^2}} - X_0\right) - \varphi'_K\left(\frac{x}{\sqrt{1-v^2}} + X_0\right) \right], \end{aligned} \quad (4)$$

where $\varphi'_{K,\overline{K}}(x) = \text{sech}^2(x)$. While v is the relative velocity between the approaching (anti)kinks, X_0 measures the initial separation up to a factor $\sqrt{1-v^2}$. We take X_0 large, so that initially we have a widely separated kink-antikink system and interference effects are absent. Then the actual value of X_0 is irrelevant. Initially kink and antikink approach each other and interact by energy exchange when they are close enough. Eventually energy is transferred to fluctuations about the kink-antikink system. This energy is then not available as translational energy and the components do not separate. Only when the fluctuations eventually release that energy again, do the kink and antikink depart. This produces so-called *bouncing* or *resonant* solutions in which kink and antikink structures partially separate but then *turn around* and approach again. The nature of the solutions varies with the initial velocity v .

2.2 Bouncing solutions and bounce windows

A typical solution to the above described initial value problem is shown in figure 1. This example exhibits the main features of the solutions to the full field equations. Kink and antikink approach each other, and rather than immediately departing to spatial infinity, they bounce and interact again before finally separating. Depending on the initial velocity several bounces may occur.

The bouncing solutions are most clearly discussed by defining a separation variable of the kink and antikink structure observed in the numerical simulation. We identify this to be the position of the antikink and we extract it as the expectation value of the coordinate along the positive half-line [10]

$$\langle x \rangle_t = \frac{\int_0^\infty dx x \epsilon(t, x)}{\int_0^\infty dx \epsilon(t, x)}. \quad (5)$$

Here

$$\epsilon(t, x) = \frac{1}{2} \left[\dot{\varphi} + \varphi'' + (\varphi^2 - 1)^2 \right] \quad (6)$$

is the classical energy density from the time dependent numerical solution to Eq. (3) with initial conditions given in Eq. (4).

Typical results for $\langle x \rangle_t$ are shown in figure 2. Essentially three types of structures are observed. At low initial velocity, kink and antikink approach and bounce several

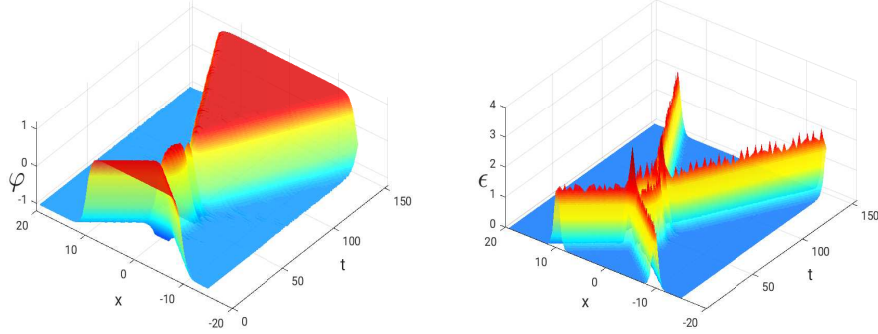


Fig. 1. (Color online) Typical solution to the initial value problem defined through equations (4) and (3) for $v = 0.251$ for the field φ in the left panel and the energy density ϵ from Eq. (6) in the right panel.

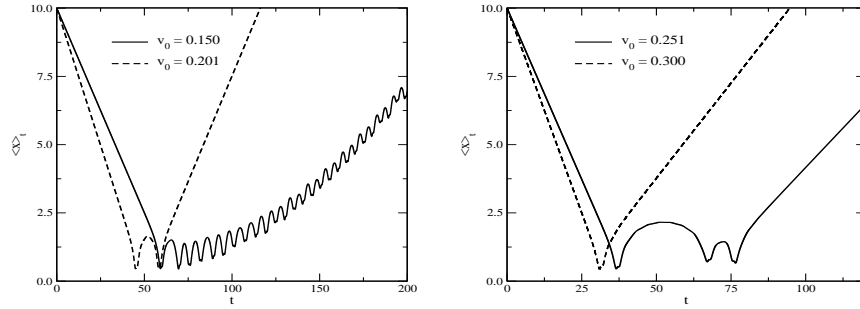


Fig. 2. Separation between kink and antikink extracted from the solutions to the partial differential equation (3) according to Eqs. (5) and (6) for different initial velocities.

times before they eventually separate. Even after separation the relative fluctuations diminish only gradually and the distinct kink and antikink configurations can be observed only for very late times. At moderate velocities, the kink-antikink system bounces a few times and then separates at slightly lower velocity. That is, at late times some of the energy remains in fluctuation modes. At large velocities the system separates without any bounce, but still some energy is contained in fluctuations about the individual (anti)kink as can be seen from the final velocity being smaller than the initial. It is obvious that at large relative velocities there is always sufficient energy available for immediate separation.

These bounce structures of the kink-antikink interaction have been exhaustively discussed in Refs. [11–15] and reviewed in Ref. [16]. In particular the critical velocity

above which no bounces occur has been extracted to be $v_c = 0.260$ [11, 12]. Also certain intervals for the initial velocity below v_c , so-called bounce windows, have been identified in which zero, one, two or any larger number of bounces occurs before the final separation.

3 Collective coordinates

We want to gain a deeper understanding of the rich bounce structures observed in the solutions to the partial differential equations. It is particularly challenging to identify those modes in which the energy is temporarily stored preventing the kink and antikink to separate immediately. For this purpose we want to model those solutions by admitting only particular modes. The introduction of collective coordinate is a very promising technique for this endeavor.

3.1 Large vs. small amplitude fluctuations

There are two distinct types of fluctuations about classical localized configurations in a field theory. In the standard procedure small amplitude fluctuations, $\eta(x, t)$ are introduced (for quantization) [1]. In a first step the field is parameterized as

$$\varphi(x, t) = \varphi_{\text{cl}}(x) + \eta(x, t),$$

where $\varphi_{\text{cl}}(x)$ represents the classical configuration, as *e.g.* the kink in Eq. (2). In the second step, the Lagrangian is expanded in powers of η . The linear order vanishes when $\varphi_{\text{cl}}(x)$ solves the field equation and contributions beyond the harmonic order are omitted. This harmonic expansion is rigorous in the \hbar counting when $\eta(x, t)$ is normalized by the canonical commutation relations and produces the leading quantum corrections to properties of the classical configuration, most prominently the vacuum polarization (or Casimir) energy [17].

The spectrum of the small amplitude fluctuations is particularly interesting in the φ^4 model. Besides the translational zero mode (see below) there is a bound state below threshold (at frequency $\omega_{\text{th}} = 2$, using dimensionless variables),

$$\eta(x, t) = e^{-i\sqrt{3}t} \chi(x) \quad \text{with} \quad \chi(x) = \frac{\sinh(x)}{\cosh^2(x)}. \quad (7)$$

In the context of the kink-antikink interaction it has been conjectured that during bounces most of the energy is stored in this so-called *shape mode* [15].

However, often there are also non-harmonic modes, that is, modes that are not subject to a restoring force and thus may acquire large amplitudes. Those modes are typically parameterized by time dependent variables. These independent variables are called collective coordinates as they describe collective motions of the classical field configuration.

3.2 Identification of crucial modes

As discussed above, a number of features motivates the introduction of collective coordinates. Unfortunately, a suitable choice may be a matter of good guess. Since

the collective modes are supposed not to experience any or only a small restoring force the (would-be) zero modes of the classical configurations are good candidates. The excitation of these modes does not alter the energy. The top candidate is, of course, the translation of the localized configuration which generates its linear momentum. As a further advantage, the introduction of collective coordinates simplifies an intricate quantum field theory problem into one of quantum mechanical nature. In higher dimensions rotations (both in coordinate and internal spaces) generate good quantum numbers that are not possessed by the classical soliton. A prominent example is the Skyrme model [18] in which canonical quantization of the collective coordinates generates baryon states [19]. (For a review see Ref. [7].) This procedure can be extended to the case of approximate, or (would-be) zero modes with the symmetry violation treated in perturbation theory.

3.3 Separation as collective coordinate

For the discussion of the interaction between kink and antikink it is obvious to introduce a time dependent collective coordinate, $X(t)$, for their separation. It takes kink and antikink with opposite velocities and parameterizes the field configuration as

$$\varphi_c(x, t) = \varphi_K(\xi_+) + \varphi_{\overline{K}}(\xi_-) - 1. \quad (8)$$

where $\xi_{\pm} = \xi_{\pm}(x, t) = \frac{x}{\sqrt{1-v^2}} \pm X(t)$. Here v equals the relative velocity in the initial conditions, Eq. (4). Substituting this parameterization and integrating over the spatial coordinate x produces the Lagrange function

$$L(X, \dot{X}) = a_1(X)\dot{X}^2 - a_2(X), \quad (9)$$

with mass (a_1) and potential (a_2) functions

$$\begin{aligned} a_1(X) &= \frac{1}{2} \int_{-\infty}^{\infty} dx [\varphi'_K(\xi_+) + \varphi'_{\overline{K}}(\xi_-)]^2 \\ a_2(X) &= \frac{1}{2} \frac{1}{1-v^2} \int_{-\infty}^{\infty} dx [\varphi'_K(\xi_+) - \varphi'_{\overline{K}}(\xi_-)]^2 + \frac{1}{2} \int_{-\infty}^{\infty} dx [\varphi_c(x, t) - 1]^2, \end{aligned} \quad (10)$$

that parametrically depend on the collective coordinate X via ξ_{\pm} . These integrals can be computed analytically [12, 20, 21] and an example is detailed in the appendix of Ref. [22]. It is, however, equally efficient to calculate them numerically since the equation of motion for the collective coordinate

$$\ddot{X} = -\frac{1}{2a_1(X)} \left[\frac{da_1(X)}{dX} \dot{X}^2 + \frac{da_2(X)}{dX} \right] \quad (11)$$

must also be solved numerically. Another motivation to obtain these integrals numerically is that small variations of the parameterization, Eq. (8) can then be easily accommodated. Since the time dependence of the field configuration only comes via $X(t)$ this is an ordinary differential equation (ODE) and thus technically less challenging than the full field equations (3).

Solutions with initial velocities analog to those in equation (4)

$$X(0) = 10 \quad \text{and} \quad \dot{X}(0) = \frac{v}{\sqrt{1-v^2}} \quad (12)$$

are displayed in figure 3. Obviously these solutions do not produce any bounce structures. This is not surprising as there is only a single degree of freedom that cannot exchange energy with any other mode. The prime candidate mode to include for this energy exchange is the shape mode, Eq. (7) whose incorporation we will discuss next.

3.4 Excitation of shape mode

We now go one step further and include the amplitude of the shape mode as a collective coordinate [21, 22]

$$\varphi_c(x, t) = \varphi_K(\xi_+) + \varphi_{\bar{K}}(\xi_-) - 1 + \sqrt{\frac{3}{2}} [A(t)\chi(\xi_-) + B(t)\chi(\xi_+)] \quad (13)$$

Note that both the kink and the antikink are accompanied by shape modes. Again this parameterization is substituted into the Lagrangian and integration over the coordinate x yields the Lagrange function

$$\begin{aligned} L(X, \dot{X}, A, \dot{A}, B, \dot{B}) = & a_1(X)\dot{X}^2 - a_2(X) + a_3[\dot{A}^2 + \dot{B}^2] - a_4[A^2 + B^2] \\ & + \bar{a}_3\dot{A}\dot{B} - \bar{a}_4AB + a_5(X)[A - B] + \dots \end{aligned} \quad (14)$$

Only a few of the many terms that exhibit the essential structures have been displayed. The full Lagrange function as well as explicit expressions for the coefficient functions are listed in Ref. [23].

Complicated Euler Lagrange equations that generalize Eq. (11) are derived from Eq. (14). At $t = 0$ kink and antikink approach each other while the shape modes are not excited initially, *i.e.* $A(0) = B(0) = 0$ and $\dot{A}(0) = \dot{B}(0) = 0$. In general the amplitudes A and B are independent. However, the above listed terms, in particular the linear term involving $a_5(X)$, suggest (and that is found for the full Lagrange function) that if $A(t)$ is a solution, so is $B(t) \equiv -A(t)$. That is, initial conditions with $B(0) = -A(0)$ and $\dot{B}(0) = -\dot{A}(0)$ produce $B(t) \equiv -A(t)$. In case there is no shape mode initially it is thus sufficient to only consider $A(t)$. From now on we

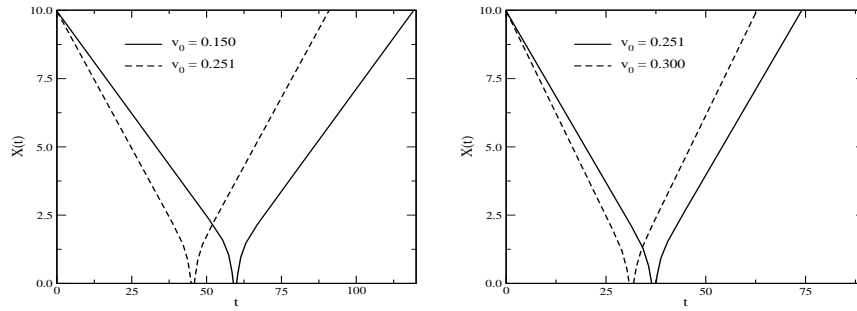


Fig. 3. Solutions to the equation of motion resulting from the collective coordinate Lagrangian, Eq. (9).

will therefore adopt that specific collective coordinate configuration. Then the shape mode part in the collective coordinate parameterization becomes [21]

$$\sqrt{\frac{3}{2}} [A(t)\chi(\xi_-) + B(t)\chi(\xi_+)] \longrightarrow \sqrt{\frac{3}{2}} [\chi(\xi_-) - \chi(\xi_+)] A(t). \quad (15)$$

As $X \rightarrow 0$ we have $\xi_- \rightarrow \xi_+$ and the coefficient of $A(t)$ vanishes. This leads to a null-vector singularity [24,25] as the amplitude is not well defined in that limit and causes a major obstacle to introducing the amplitude of the shape mode as a collective coordinate. This obstacle can only be circumvented by particular approximations or modifications.

The comparison with the (integrable) sine-Gordon soliton further motivates to consider the shape mode as the prime candidate for intermediate energy storage. That model actually lacks a shape mode type solution as a small amplitude fluctuation off the soliton. Neither do bounces occur in the soliton-antisoliton interaction as the known analytic expression [1] for the time-dependent system reveals; only some time delay or phase shift is observed in the soliton-antisoliton interaction [12]. With generalizations or additions of impurities, bounces emerge [26] that have been analyzed using collective coordinates in Refs. [27,28].

3.5 Approximations in collective coordinate calculations

Early approaches to solve the equations of motion for the collective coordinates $X(t)$ and $A(t)$ circumvented the null-vector problem by omitting the X dependences in a_3 and a_4 by equating them to their constant values from the respective $X \rightarrow \infty$ limits. Essentially this omits the interference between the two shape modes at ξ_{\pm} . Furthermore non-harmonic terms in A , *i.e.* those beyond quadratic order in the Lagrangian were discarded [14,15,25,29]. Calculations (denoted 'lit' in figure 4) based on these approximations indeed showed surprising agreement with the results from the full field equation (3). Unfortunately those calculations took $a_5(X)$ from the original paper [21] which suffers from a misprint that made its way through the literature. Correcting² the misprint [22] and re-analyzing the equations of motion using the same approximations removes any agreement with the results from Eq. (3) as displayed in figure 4. The separation coordinate turns negative with a significant modulus and wild oscillations. Only occasionally it returns to the positive regime but essentially it is trapped below zero. Obviously these approximations, in particular omitting higher powers in A , are not consistent with the results from numerically simulating the full field equations.

3.6 Orbits of collective coordinates

Comparing the numerical solutions with (Fig. 4) and without (Fig. 3) a collectively excited shape mode with that of the full solution in figure 2 suggests that this mode may indeed be significant, but that its incorporation as the only collective coordinate on top of the separation exaggerates its role. To further investigate this conjecture we scale its source by a constant γ :

² Remarkably, the fitted function $a_5(X) \propto e^{-X}$ studied in Refs. [25,29] reasonably resembles the actual behavior.

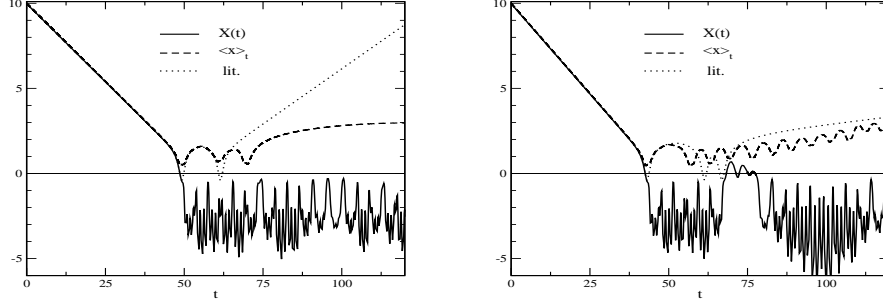


Fig. 4. Kink-antikink separation as function of time. Collective coordinate calculation of Eqs. (13) and (15): full lines; field equations: dashed lines; collective coordinate approach from Refs. [14, 15]: dotted lines. Left panel: $v = 0.184$; right panel $v = 0.212$.

$$a_5(X) \longrightarrow \gamma a_5(X) \quad (16)$$

and again solve the equations of motions within the above discussed approximations. The resulting time dependences for both the separation X and the shape mode amplitude A are displayed in figure 5. We see that a moderate rescaling produces

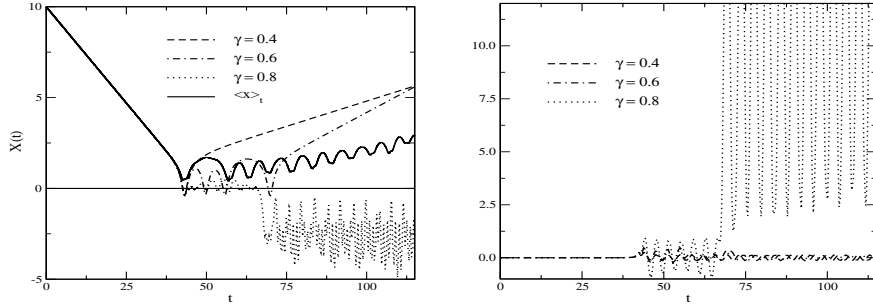


Fig. 5. Collective coordinates from scaled source, Eq. (16) for $v = 0.212$ in the harmonic approximation.

trajectories for $X(t)$ that compare reasonably well with $\langle x \rangle_t$ extracted from the full field equations. For small γ the bounce structure disappears (*cf.* Sec. 3.3) while taking the source with full strength produces too large amplitudes for the shape mode and ties the separation coordinate into the negative domain. However, even for $\gamma = 0.5$ we find the critical velocity to be about $v_c = 0.33$ which is significantly larger than the value extracted from the exact solution. This suggests that, though the shape plays a significant role, other modes seem equally relevant.

Note, however, that these are intermediate conclusions, as the collective coordinate approach has been furnished by a number of approximations. We will elaborate on these approximations in the following section.

4 Comments on approximations

In the previous section we have seen that, in the context of kink-antikink scattering, frequently adopted approximations within the collective coordinate formulation do not reproduce the results from the field equations. It is therefore suggestive that a better agreement will be obtained when these approximations will be abandoned.

Most of the approximations for the collective coordinate approach have been implemented to gain simplifications that lead to analytic results or to avoid technical problems. With a fully numerical approach, some of these approximations can easily be abandoned.

4.1 Non-harmonic contributions

When omitting the non-harmonic contributions of the shape mode amplitude, the collective coordinate equations of motion can be utilized to analytically predict the critical velocity [15, 21]. One may also argue for their omission on the basis that the shape mode as bound state in the background of a single kink results from exactly that approximation. However, the results shown in figure 5 are actually inconsistent with the harmonic approximation. It is obvious that the amplitude of the shape mode may be large and therefore $\mathcal{O}(A^2)$ terms may not be omitted from the equations of motion. Inclusion of these higher order terms may hamper the amplitude of the shape mode from becoming large by absorbing a significant amount of energy. In turn this might improve the quality of collective coordinate approach. Stated otherwise, the non-harmonic terms are hoped to assist towards reducing the amplitude A such that the small amplitude approximation, which introduced the shape mode in the first place, is indeed justified.

4.2 Null-vector singularity

We have already mentioned that the collective coordinate parameterization of Eq. (15) produces an ill-defined amplitude of the shape mode when $X \rightarrow 0$ for the solution with $A(t) = -B(t)$ which is realized when the initial conditions obey this relation. To show that this holds true even without the identification $A \equiv -B$ we consider the kinetic terms involving the shape mode. The associated coefficients are

$$a_3(X) = \frac{3}{4} \int dx \chi^2(\xi_{\pm}) = \frac{3}{4} \sqrt{1-v^2} \int dx \chi^2(x) \text{ and } \bar{a}_3(X) = \frac{3}{2} \int dx \chi(\xi_+) \chi(\xi_-). \quad (17)$$

When $X = 0$ we have that $\xi_+ = \xi_- = \frac{x}{\sqrt{1-v^2}}$ so that $\bar{a}_3(0) \rightarrow 2a_3(0)$. Then the coefficient matrix in the collective coordinate Lagrangian becomes

$$\begin{pmatrix} a_3(X) & \bar{a}_3(X) \\ \bar{a}_3(X) & a_3(X) \end{pmatrix} \sim a_3(0) \begin{pmatrix} 1 & 1 \\ 1 & 1 \end{pmatrix},$$

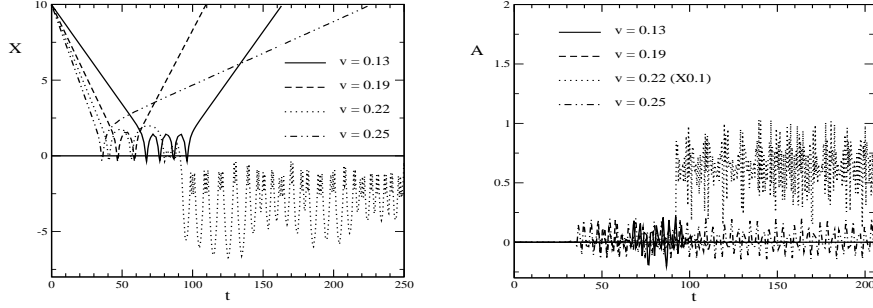


Fig. 6. Solution to the collective coordinate equations of motion in the φ^4 model. Left panel: kink-antikink separation, right panel: amplitude of shape mode (note the change of scale in the $v = 0.22$ entry).

whose null-vector $\begin{pmatrix} 1 \\ -1 \end{pmatrix}$ is indeed the solution $A(t) = -B(t)$ [24]. The above matrix cannot be inverted and it becomes impossible to formulate the equations of motion as $\ddot{A} = \dots$ and $\ddot{B} = \dots$. The potential part containing $a_4(0)$ and $\bar{a}_4(0)$ has the same null-vector. In the numerical approach this singularity allows arbitrarily large amplitudes of the shape mode when $X \sim 0$. This suggests to modify the collective coordinate parameterization such that $X \rightarrow 0$ is energetically disfavored. We will get back to this in the next section.

4.3 Disagreement with solution to field equations

In view of the above discussion it is therefore suggestive to solve the collective coordinate equations as they emerge from the Lagrange function, Eq. (14) for $X(t)$ and $A(t) (= -B(t))$. At this point the sole approximation is to omit $\bar{a}_3(X)$ and $\bar{a}_4(X)$ (that is, keep the coefficients of the harmonic terms at their $X \rightarrow \infty$ values) to avoid the technical null-vector problem discussed above. The results of these calculations are shown in figure 6. It turns out that the energy associated with the source term for the shape mode, $E_5 = -a_5(X)A$, may absorb much energy when X becomes negative and trapping type solutions with large amplitudes of the shape mode emerge. Hence the inclusion of the non-harmonic terms does not produce an a posteriori justification for implementing the harmonic approximation. The entry with $v = 0.22$ in figure 6 is a typical example thereof.

To further reflect on the quality of the collective coordinate formulation we again apply the scaling of Eq. (16) to one of the worst results to this case. The resulting time dependence of the separation variable is shown in figure 7. Obviously there is quite a sensitivity with respect to the strength of the source term. It is unlikely that the collective coordinate approach is sensitive enough to properly account for such fine details. This also concerns the predictions for the outgoing velocities.

Most notably, however, we find that without the many approximations (and $\gamma = 1$), the collective coordinate approach predicts a critical velocity of $v_c = 0.247$ above which trapping or bounce type solution cease to exist. This still compares

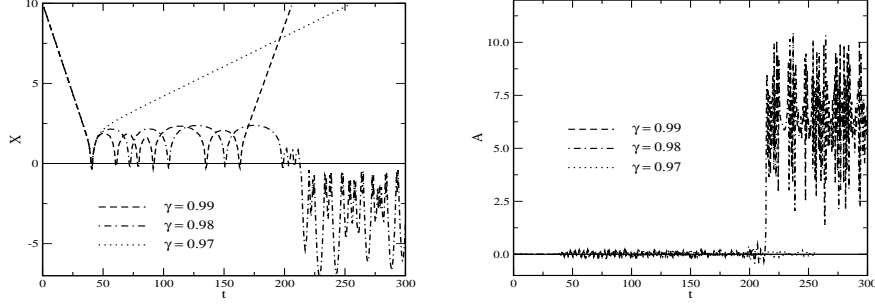


Fig. 7. Collective coordinates from scaled source, Eq. (16) for $v = 0.22$.

favorably to the result from the full field equations of 0.260 [11,12]. Yet, in view of the various discrepancies between the two approaches below v_c , this may be a mere artifact.

5 Modifications

Obviously negative $X(t)$, in particular with a large modulus, should not appear³. We have seen that when $X(t)$ is trapped at (large) negative values, even with the non-harmonic terms included, the amplitude of the shape mode contradicts the assumption for the small amplitude approximation which has been the point of departure for the shape mode and its subsequent use as collective coordinate.

Originally, taking X as a collective coordinate was motivated from the configuration containing widely separated kink and antikink structures. Of course, such a starting point does not determine a unique collective coordinate parameterization as we can always add any contribution that vanishes as $X \rightarrow \infty$. Here we will explore one such modification.

5.1 Kink-antikink penetration

The collective coordinate parameterization of Eq. (8) turns into a vacuum configuration of zero energy when $X \sim 0$. This causes attraction for small and moderate separation and eventually produces solutions that are trapped with negative X and correspond to (un-desired) configurations in which kink and antikink have penetrated each other. We thus modify the collective coordinate description and introduce a variational parameter q

³ The comparison with the solutions to the full field equations proceeds via $\langle x \rangle_t$ which is positive definite, *cf.* Eq. (5). Hence any such comparison is bound to fail for negative $X(t)$. We will therefore also consider the actual field configurations in section 5.4.

$$\varphi_c(x, t) = \varphi_K(\xi_+) + \varphi_{\bar{K}}(\xi_-) - \tanh(qX) + \sqrt{\frac{3}{2}}A(t) [\chi(\xi_-) - \chi(\xi_+)] . \quad (18)$$

For $q \gg 1$ this agrees with the original formulation, Eq. (8) when $X \geq 0$ which embraces the desired initial condition. In contrast to Eq. (8), however, it is also a solution to the field equations when $X \rightarrow -\infty$ (with $A = 0$). Actually the configuration, Eq. (18) is anti-symmetric under $X \rightarrow -X$.

With the $\tanh(qX)$ term, the $X \sim 0$ configuration ceases to be a vacuum configuration. In turn this produces a repulsive potential, $a_2(X)$ for $X \rightarrow 0$. When q is large, the repulsion resembles a peak on top of the intermediate attraction of the original parameterization. For moderate and small q it essentially removes that attraction. This scenario is pictured in figure 8.

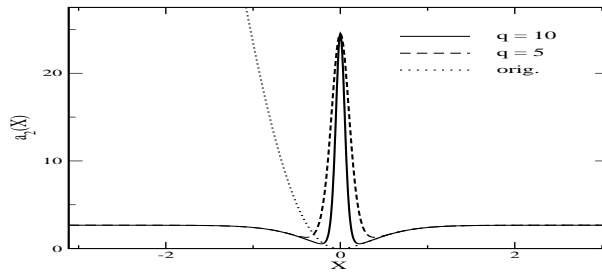


Fig. 8. Potential for the separation collective coordinate from the modified parameterization, Eq. (18) with $v = 0.2$. The entry 'orig.' refers to the background of Eq. (8).

We note that the parameterization, Eq. (18) is different from the one used in Ref. [22] since here we immediately impose equal amplitudes for the two shape modes via Eq. (15). Though that equality also results from the equations of motion associated to Eq. (18), various approximation/modifications may yield different numerical results (Most of the numerical simulations in Ref. [22] assumed the $X \rightarrow \infty$ values for the harmonic terms.)

There is no fundamental principle in choosing a value for q other than Eq. (18) initially resembles a well separated kink antikink system, *i.e.* $qX_0 \gg 1$. Later we will see that there is not much variation in the structure of the soliton with q once it is taken large enough. A guiding principle to select q could, for example, be to tune it for any given value of v such as to achieve maximal agreement with the solution from the field equations. This was done in Ref. [30], however in the context of the ϕ^6 model, *cf.* section 6.

5.2 Improved agreement with solution to field equations

We discuss the numerical solutions for the collective coordinate description of Eq. (18) and compare typical results with those from the full calculation in figure 9. The two graphs on top originate from taking the coefficients of the quadratic

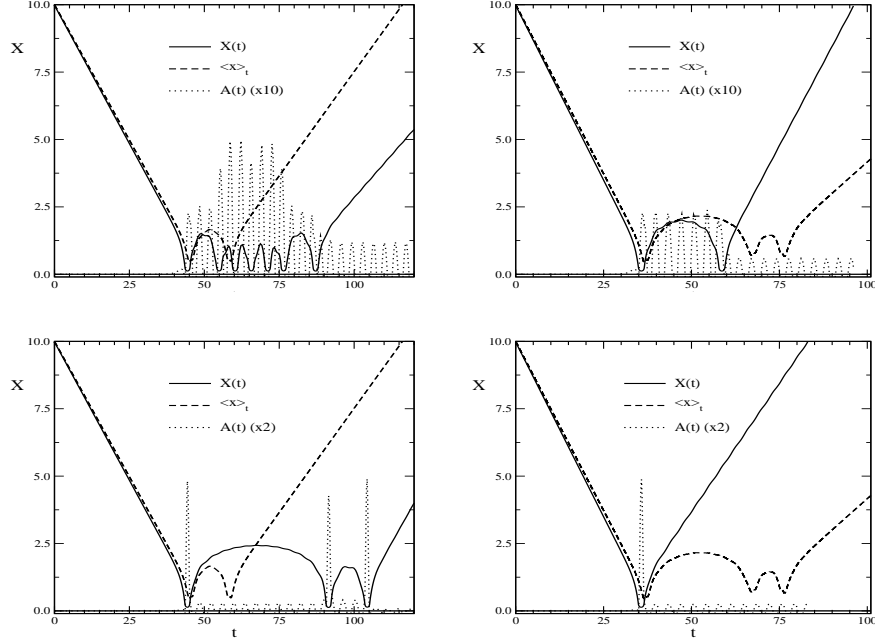


Fig. 9. Collective coordinate calculations with $q = 10$ in Eq. (18) with all terms from the collective coordinate Lagrangian included. Top graphs: Coefficients of harmonic terms kept constant at their $X \rightarrow \infty$ values. Bottom graphs: X dependence of harmonic terms included. Left panel: $v = 0.201$, right panel: $v = 0.251$. Note the different scales for $A(t)$.

terms, both for the kinetic (a_3) and the potential (a_4) constants at their $X \rightarrow \infty$ values. This approximation is adapted from earlier attempts to avoid the null-vector problem. We see that this collective coordinate approach indeed describes a finite number of bounces and that these bounces come together with measurable excitations of the shape mode. However, neither the number of bounces nor the time scale at which these bounces occur are properly reproduced by the collective coordinate calculation. Also there is no systematic in the deviation as, for example, that the collective coordinate approach would always underestimate the number of bounces or that it would always predict too large a time interval during which bounces occur.

The results shown in the two bottom pictures of figure 9 abandon all approximations. In that case the null-vector problem may occur. However, numerically this does not happen. For the cases displayed in figure 9 we always find that $X \geq 0.1$. Of course, this value is correlated to $1/q$ that characterizes the regime of the short range repulsion. Though the substitution $1 \rightarrow \tanh(qX)$ affects the coefficients $a_i(X)$ only in the moderate regime $|X| \lesssim 3$, significant changes for $X(t)$ and $A(t)$ are measured. Yet, the number of changes as well as the interaction times vary with v and q . Thus much of the predictive power of these calculations is lost.

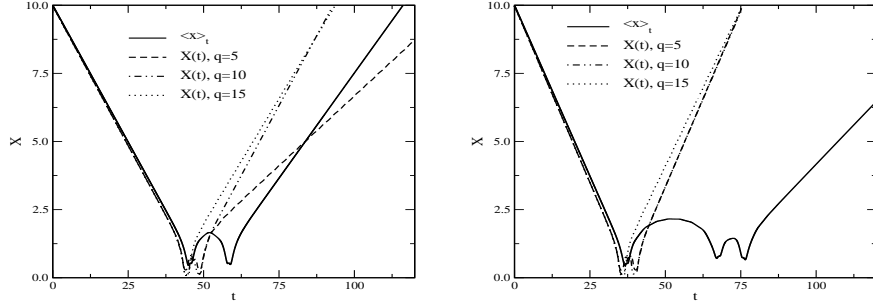


Fig. 10. Effect of tuning q in Eq. (18) for two velocities, $v = 0.201$ (left panel) and $v = 0.251$ (right panel).

It has become apparent that the quality of the collective coordinate approach strongly depends on the applied approximations and no rigorous conclusion can be drawn. Similar to Ref. [30] one might consider the new parameter q a tunable variable. Results for such simulations are compared to the mean value of the full solution in figure 10. While there are some variations with q , the main structure of several bounces over a long time interval cannot be adjusted.

5.3 Extraction of critical velocities

Once kink and antikink start to separate, the major share of the energy is stored in the translational motion. This raises expectations that the predictions for the critical velocities above which no bounces occur agree for the two approaches. However, this is only partially the case. The exact value for the critical velocity from the field equations of 0.260 [11, 12] is underestimated within the collective coordinate approach of Eq. (18) to be 0.204 when $q = 10$. However, that particular value again changes with q . For example, bounces are observed for $v = 0.4$ when $q = 5$.

We compare the initial and final velocities above critical velocities as extracted from $\frac{\partial \langle x \rangle_t}{\partial t}$ and $\dot{X}_\infty = \frac{\partial X(t)}{\partial t}$ as $t \rightarrow \infty$. Subsequently the collective coordinate velocity is written in relativistic kinematics $v_f = \frac{\dot{X}_\infty}{\sqrt{1 + \dot{X}_\infty^2}}$. Since there are still oscillations of the shape mode on top of the translation those velocities are not constant and the results listed in table 1 are obtained from averaging over numerous such oscillations. Again we see that the collective coordinate approach reproduces the exact results only qualitatively and that particularities (here represented by a strong q dependence) matter. We also observe from the PDE entry of table 1 that for large initial velocities the full field equations predict reduced final velocities. That is, even without bounces, some energy is stored in modes other than the translation.

v	PDE	coll. coord.		
		$q = 5$	$q = 10$	$q = 15$
0.4	0.279	0.216	0.399	0.340
0.5	0.390	0.447	0.496	0.404
0.6	0.494	0.569	0.577	0.388
0.7	0.595	0.700	0.612	0.699
0.8	0.697	0.818	0.806	0.808
0.9	0.797	0.897	0.879	0.906

Table 1. Comparison of the predicted final velocities, v_f . The entry PDE refers to $\frac{\partial \langle x \rangle_t}{\partial t} \Big|_\infty$ and the q columns contain \dot{X}_∞ originating from Eq. (18).

5.4 Mapping collective coordinates and solution to full field equation

By pure definition, Eq. (5) $\langle x \rangle_t$ is non-negative. Thus a direct comparison with $X(t)$ may be misleading. We therefore attempt to rebuild the time dependent field from Eq. (18) with $q = 10$ by substituting $X(t)$ and $A(t)$ and then compare that configuration to the solution from the field equations, Eq. (3) with the same initial velocity.

We analyze the (dis)agreement in two ways. First, in figure 11 we consider the field at the center ($x = 0$) as a function of time and, second, we contrast the configurations along the coordinate axis at different times in figure 12. As in figure 9 (with $v = 0.201$) we observe that the time between the first two collisions of kink and antikink is overestimated by the collective coordinate description. We also see that the collective coordinate approach yields two nearby bounces at late times when the field equations predict well separated kink-antikink structures. Similarly the number and positions of bounces are not correct for $v = 0.251$ either. Interestingly enough, the collective coordinate result for $v = 0.201$ agrees in shape (though not with respect to the time scale) with the exact result of $v = 0.251$. This again suggests

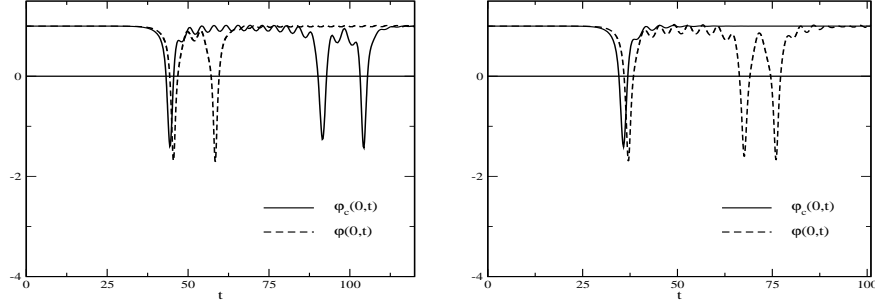


Fig. 11. Time dependence of the field at the origin. Left panel: $v = 0.201$, right panel: $v = 0.251$. Collective coordinate results are without any approximation, *i.e.*, similarly to the bottom graphs of figure 9.

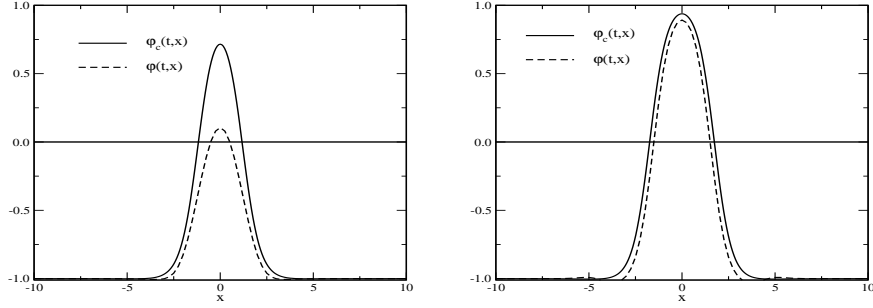


Fig. 12. Fields at different times for $v = 0.201$. Left panel: $t = 47$, right panel: $t = 50$.

that details of the parameterization matter and that the velocities should not be literally compared.

A further striking difference between the two approaches seen in figure 12 is that, at particular times, the peak amplitudes of the field configurations differ significantly. Of course, this just reflects that at those particular times which exhibit significant differences one approach produces a bounce but the other does not.

6 Comparison: ϕ^6 model

Without going into much detail we briefly reflect on related studies within the ϕ^6 model. It is interesting because bounce structures have been observed for the solutions to the field equations (analog to Eq. (3)) [31] even though no internal shape mode exists in the fluctuation spectrum of the soliton(s). This is a further indication that the shape mode is not the (only) explanation for bounces in kink-antikink scattering.

This model is defined by the (scaled) Lagrangian

$$\mathcal{L}_6 = \frac{1}{2} [\dot{\phi}^2 - \phi'^2] - \frac{1}{2} (\phi^2 + a^2) (\phi^2 - 1)^2, \quad (19)$$

with the real parameter a . For $a \neq 0$ there are two vacua $\phi_{\text{vac}} = \pm 1$ and the soliton solution mediates between them. We will only consider the $a = 0$ case when an additional vacuum, $\phi_{\text{vac}} = 0$ emerges. Then the soliton solutions

$$\phi_{K, \bar{K}}(x) = [1 + \exp(\pm 2x)]^{-\frac{1}{2}} \quad (20)$$

mediate between 0 and 1 (or -1 when changing the overall sign). The small amplitude bound state spectrum for both solitons only contains the translational zero mode.

With two distinct soliton solutions available there are two independent initial conditions that relate to interactions between kink and antikink. They are usually referred to as kink-antikink ($K\bar{K}$) and antikink-kink ($\bar{K}K$) systems and the full field equations produce bounce structures for both systems [31].

Though there is no shape mode in the spectrum of the small amplitude fluctuations its inclusion as in Eq. (15) may serve as working hypothesis for the collective coordinate approach to analyze the temporal storage of energy during the bounces. Furthermore a Fourier analysis of $\phi(0, t)$, the solution of the field equations at the origin, in the $\overline{K}K$ system shows large amplitudes at frequencies below threshold [31], suggesting that the energy is indeed stored in localized modes. Studies based on this hypothesis have been reported in Refs. [10, 22] and we reproduce typical results for the $K\overline{K}$ and $\overline{K}K$ systems in figures 13 and 14, respectively. Again, the null-vector problem has been circumvented by approximating the coefficients of the terms quadratic in A by their asymptotic values. As is by now standard, $\langle x \rangle_t$ has been extracted via Eq. (5) from the time dependent energy density deduced from Eq. (19) with $a = 0$. For $v \leq 0.289$ the $K\overline{K}$ is always trapped [31]. Above that velocity the two structures always reflect without any bounce. With the separation as the only collective coordinate the former feature can, by construction, not be reproduced. (See Ref. [30] for more details on this modification.) Calculations with the shape mode added are shown in figure 13. Solutions with bounces are now produced for small enough velocities. In contrast to the full solution, however, trapping does typically not occur in the collective coordinate method. Neither is this accomplished by modifications similar to Eq. (18) [22, 23] though the bounces are maintained by those modifications. On the other hand, for larger velocities the two calculations yield similar results.

In figure 14 the two methods are compared for the $\overline{K}K$ system for which the critical velocity is much smaller: $v_c = 0.046$ [31]. There are obvious discrepancies below that velocity, while agreement is again observed for larger values.

Interestingly enough despite all the obstacles observed, the ordering relations for the critical velocities

$$v_c(\phi^6, \overline{K}K) \ll v_c(\phi^4, K\overline{K}) \lesssim v_c(\phi^6, K\overline{K})$$

in the different models are nevertheless observed in both the exact and the collective coordinate approaches [22]. The first relation is expected because those velocities differ by an order of magnitude and even a coarse approximation should reproduce it. The second relation may be a mere artifact.

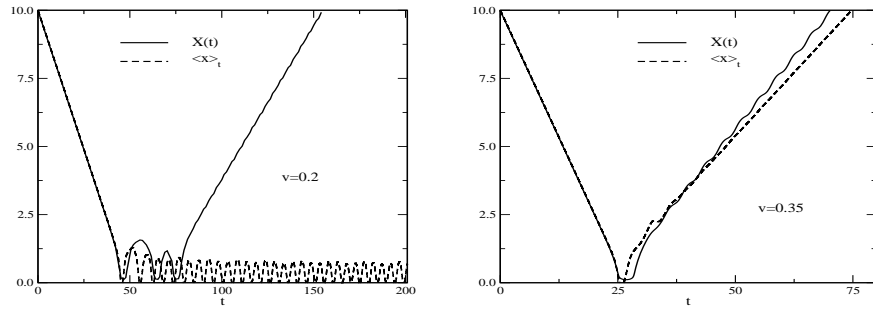


Fig. 13. Kink-antikink scattering in the ϕ^6 model: comparison of full and collective coordinate solutions for particular initial velocities.

7 Conclusion and critical analysis

The ϕ^4 model in one space and one time dimensions has localized static solutions, so-called (anti)kinks. Appropriate initial conditions for integrating the full field equations allow to simulate kink-antikink scattering as a prototype of particle interactions in the soliton picture. A number of interesting features emerge from these simulations as the relative initial velocity is varied. In particular, below a critical velocity (multiple) bounces occur between kink and antikink.

The collective coordinate method has been introduced as (i) a manageable approximation to the full field equations to simplify partial to ordinary differential equations and (ii) a sensible means to identify important modes in the kink-antikink interaction. In particular the degrees of freedom that are bound states of the single soliton have been considered. In the case of the ϕ^4 model these are the translational zero mode and so-called shape mode.

Here we have confronted the collective coordinate method with the exact treatment of the field equations in the ϕ^4 model. The collective coordinate approach reproduces well the first bounce observed in kink antikink collisions. This remarkably includes the acceleration shortly before kink and antikink sit on top of each other. However, when the separation is tiny, the non-linear equations of motion are particularly sensitive to small changes and the detailed pattern cannot be accommodated by the collective coordinate approach.

In fact, straightforward implementations of collective coordinates do not produce acceptable agreement with the solutions of the field equations. Intricate adjustments are needed to improve on the solutions. Even then significant discrepancies emerge. It is thus difficult to draw conclusions from the collective coordinate approach on the relevance of particular excitations, at least quantitatively.

Qualitatively the collective coordinate approach to some extent supports the conjecture that energy storage in the shape mode excitation leads to bouncing kink-antikink configurations. However, in that approach the amplitude of the shape mode is inflated compared to the exact solution. This suggests that other modes play a decisive role as well. It is also important to mention that within the interaction regime, *i.e.* when the distance between kink and antikink is not large, the shape mode ceases to be a solution to the fluctuation spectrum of φ_{cl} . Though considering

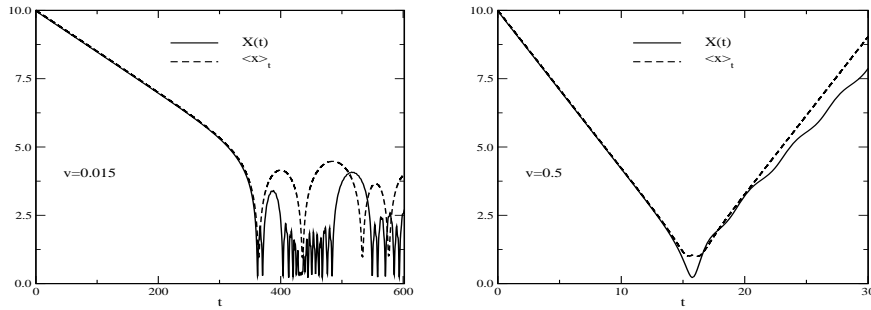


Fig. 14. Same as Fig. 13 for antikink-kink scattering in the ϕ^6 model.

the linearized field equations is fully consistent only when the background is an extremum of the action - the kink-antikink system is not - it may clarify whether the shape mode maintains its unique role from the single kink system. Such studies [32, 33] show that the fluctuation spectrum of two (even widely) separated, stationary (anti)kinks differs significantly from that of a single kink. For fixed $X \gtrsim X_c \approx 0.37$ the zero mode acquires negative frequency squared, indicating instability since two localized (anti)kinks at finite separation do not solve the field equations. On the other hand, for $X \lesssim X_c$ the shape mode ceases to be bound which questions its incorporation as collective mode from the beginning. Also, the shape mode is a solution within the small amplitude approximation for deviations from a single kink. Smallness of this amplitude is not supported by the collective coordinate approach. (When computing scattering phase shifts about a single kink from the full non-linear field equations, amplitudes as small as $A \sim 0.1$ yield results that deviate from the small amplitude approximation [34].) Hence most of the arguments leading to the incorporation of the shape mode are not rigorous in the regime of kink-antikink interactions. Another major issue in comparing the solutions of the two approaches is the fact that the relative velocities between the outgoing kink and antikink do not exactly match. This is most apparent from the different slopes of $X(t)$ and $\langle x \rangle_t$ in the above figures.

In conclusion, we see that though the shape mode has its share in producing bouncing configurations in the kink-antikink scattering, the collective coordinate approach based on this mode is not sensible enough to reproduce the scattering process quantitatively. It is thus very likely that other modes are equally relevant for the temporary storage of energy. To clarify whether these are just a few modes one could perform a thorough Fourier analysis in space and time of the difference

$$\varphi(x, t) - [\varphi_{\overline{K}}(x - \langle x \rangle_t) + \varphi_K(x + \langle x \rangle_t) - 1] ,$$

with $\langle x \rangle_t$ computed via Eq. (5) from $\varphi(x, t)$, the solution from the field equations. The result from that analysis may motivate more suitable collective coordinate parameterizations.

Acknowledgments

The author gratefully acknowledges helpful contributions from A.M.H.H. Abdelhady and I. Takyi. This work is supported in part by the National Research Foundation of South Africa (NRF) by grant 109497.

References

1. R. Rajaraman, *Solitons and Instantons*, (North Holland, Amsterdam 1982).
2. Y. T. Kivshar, B. A. Malomed, Rev. Mod. Phys. **61** (1989) 763 Addendum: [Rev. Mod. Phys. **63** (1991) 211].
3. T. Vachaspati, *Kinks and domain walls: An introduction to classical and quantum solitons* (Cambridge University Press, 2010).
4. A. Vilenkin, E. P. S. Shellard, *Cosmic Strings and Other Topological Defects* (Cambridge University Press, 2010).

5. B. Ivanov, A. Kichiziev, Y. N. Mitsai, Sov. Phys. JETP **75** (1992) 319.
6. A. R. Bishop, J. A. Krumhansl, S. E. Trullinger, Physica, **D1** (1980) 1.
7. H. Weigel, Lect. Notes Phys. **743** (2008) 1.
8. N. S. Manton, P. Sutcliffe, *Topological solitons* (Cambridge University Press, 2004)
9. R. Vinh Mau, M. Lacombe, B. Loiseau, W. N. Cottingham, P. Lisboa, Phys. Lett. **150B** (1985) 259.
10. H. Weigel, J. Phys. Conf. Ser. **482** (2014) 012045.
11. M. Moshir, Nucl. Phys. B **185** (1981) 318.
12. D. K. Campbell, J. F. Schonfeld, C. A. Wingate, Physica **9D** (1983) 1.
13. T. I. Belova, A. E. Kudryavtsev, Physica D **32** (1988) 18.
14. P. Anninos, S. Oliveira, R. A. Matzner, Phys. Rev. D **44** (1991) 1147.
15. R. H. Goodman, R. Haberman, SIAM J. App. Dyn. Sys. **4** (2005) 1195.
16. T. I. Belova, A. E. Kudryavtsev, Phys. Usp. **40** (1997) 359 [Usp. Fiz. Nauk **167** (1997) 377].
17. N. Graham, M. Quandt, H. Weigel, Lect. Notes Phys. **777** (2009) 1.
18. T. H. R. Skyrme, Proc. Roy. Soc. Lond. A **260** (1961) 127.
19. G. S. Adkins, C. R. Nappi, E. Witten, Nucl. Phys. B **228** (1983) 552.
20. A. E. Kudryavtsev, JETP Lett. **22** (1975) 82.
21. T. Sugiyama, Prog. Theor. Phys. **61** (1979) 1550.
22. I. Takyi, H. Weigel, Phys. Rev. D **94** (2016) 085008.
23. I. Takyi, *Collective coordinate description of kink-antikink interaction*, <http://scholar.sun.ac.za/handle/10019.1/97877> MSc Thesis, Stellenbosch University (2016), unpublished.
24. J. G. Caputo, N. Flytzanis, Phys. Rev. A **44** (1991) 6219.
25. R. H. Goodman, R. Haberman, Phys. Rev. Lett., **98** (2007) 104103.
26. M. Peyrard, D. K. Campbell, Physica **9D** (1983) 33.
27. Z. Fei, Y. S. Kivshar, L. Vázquez, Phys. Rev. A **45** (1992) 6019.
28. R. H. Goodman, R. Haberman, Physica D **194** (2004) 303.
29. R. H. Goodman, A. Rahman, M. J. Bellanich, C. N. Morrison, Chaos **25** (2015) 043109.
30. A. Demirkaya, R. Decker, P. G. Kevrekidis, I. C. Christov, A. Saxena, JHEP **1712** (2017) 071.
31. P. Dorey, K. Mersh, T. Romanczukiewicz, Y. Shnir, Phys. Rev. Lett. **107** (2011) 091602.
32. Z. Lee, *Quantum corrections to the kink-antikink potential*, <http://scholar.sun.ac.za/handle/10019.1/100796>, MSc Thesis, Stellenbosch University (2017), unpublished.
33. N. Graham, R. L. Jaffe, Phys. Lett. B **435** (1998) 145.
34. A. M. H. H. Abdelhady, H. Weigel, Int. J. Mod. Phys. A **26** (2011) 3625.